Charge inhomogeneities due to smooth ripples in graphene sheets

Fernando de Juan, Alberto Cortijo, and María A. H. Vozmediano
Unidad Asociada CSIC-UC3M, Instituto de Ciencia de Materiales de Madrid, CSIC, Cantoblanco, E-28049 Madrid, Spain
(Received 14 June 2007; revised manuscript received 22 August 2007; published 8 October 2007)

We study the effect of the curved ripples observed in the freestanding graphene samples on the electronic structure of the system. We model the ripples as smooth curved bumps and compute the Green's function of the Dirac fermions in the curved surface. Curved regions modify the Fermi velocity that becomes a function of the point on the graphene surface and induce energy dependent oscillations in the local density of states around the position of the bump. This effect is due to the change of the Pauli matrices with the position and is independent of the well known gauge potential generated by the spin connection. The corrections to the density of states are only due to the first effect and are estimated to be of a few percent of the flat density of states. Local probes such as scanning tunnel microscopy should be able to observe the predicted correlation of the morphology with the electronics. We discuss the connection of the present work with a recent observation of charge anisotropy in graphene and argue that the ripples can provide an alternative explanation.

DOI: 10.1103/PhysRevB.76.165409 PACS number(s): 81.05.Uw, 75.10.Jm, 75.10.Lp, 75.30.Ds

I. INTRODUCTION

Recent experiments of transmission electron microscopy (TEM)[1,2] show that the suspended graphene samples exhibit an apparently random spontaneous curvature that can be visualized as ripples of various sizes that can reach a few angstroms high and several nanometers long. Observed ripples have also been reported later in scanning tunneling microscopy[3,4] (STM). The issue of curvature of graphene and its possible influence on the electronic properties have been addressed before. Inspired by the physics of nanotubes and fullerenes most of the works done on the electronic properties of curved graphene dealt with curvature induced by topological defects.[5–9] In these works it was shown that conical singularities in the average flat graphene sheet induce characteristic charge anisotropies that could be seen in STM or TEM. Charge anisotropies in monolayer graphene have been recently observed in scanning single electron transistor experiments[10] that show a distribution of electron-hole puddles at the Fermi level which could be responsible for the minimal conductivity of graphene.[11] Charge anisotropies have also been reported in electrostatic force microscopy experiments done in graphite.[12] Charge inhomogeneities in graphene have been computed recently associated with impurity states[13] or elastic strain[14] of a nature very similar to the one obtained previously with topological defects. It is by now clear that fluctuations in structure and charge are closely related and it seems that most types of disorder will induce charge anisotropies near the Dirac cone.

In this work we study the effect of smooth curved portions of the type described in the experiments on the density of states of graphene by coupling the Dirac equation describing the low energy electronic properties of graphene to a general metric describing a smooth curved piece in the average flat surface. The formalism is the same used in Refs. 8 and 9 to study the effect of pentagon and heptagon rings but here there are no curvature singularities. We obtain that the charge density couples to the shape of the graphene surface. The local density of states oscillates with the energy and the maximal correction has a spacial extent of the order of the defect. The estimated value of the relative correction at the typical energies explored in the experiments can be of the order of a few percent of the flat value much bigger than the one obtained with elasticity models. The predicted correlation of the morphology of the sample with the electronics should be observed in local probes as STM or TEM experiments. The present mechanism can explain qualitatively the recent observations of charge inhomogeneities at zero energy found in graphene[10] as due to the space variation of the Fermi velocity induced by the curvature.

This paper is organized as follows: Section II explores the consequences of coupling the two-dimensional Dirac Hamiltonian to a curved surface using a smooth Gaussian bump as an example. At this level we see that as a consequence of the curvature two independent things happen: the Fermi velocity acquires a nontrivial dependence on the position, and a gauge field is generated. Section III is devoted to the computation of the local density of states of the system. We first describe the effects of the curvature in terms of an effective potential and then compute the electron Green's function in the curved space to first order in perturbation theory. The perturbative parameter is related to the deviation of the graphene surface from the flat plane. Section IV analyzes the results. In Sec. V we discuss the possible experimental consequences that can be extracted from this work, in particular, in connection with the anisotropies of Ref. 10. In Sec. VI we present the conclusions and discussion. The Appendix is devoted to the definition and computation of the various geometrical factors associated with the problem.

II. TWO-DIMENSIONAL DIRAC EQUATION IN A CURVED SPACE WITH POLAR SYMMETRY

The most obvious way to study the effects of the topography of the sample on the electronic degrees of freedom is to couple the Dirac equation that governs the low energy electronics to the curved surface. This approach has been applied to study curved fullerenes[15–19] and to compute the response of electromagnetic charges to conical defects in

planar graphene[20] in the framework of the equivalence between the theory of defects in solids and the three-dimensional gravity.[21,22] The coupling of the electronic degrees of freedom of planar graphene to conical defects has been explored in Refs. 8, 9, and 23. There it was found that a distribution of pentagons and heptagons induces characteristic inhomogeneities in the density of states of the graphene surface. In order to investigate the effect of pure curvature on the electronic properties of graphene, the conical defects studied previously present two difficulties. First they correspond to surfaces with zero intrinsic curvature; moreover the extrinsic curvature is accumulated at the apex of the cone where the surface has a singularity. It is then not clear if the results obtained—which look similar to the ones got with vacancies in Ref. 13—are due to the singularity or to the curvature. To disentangle the two effects we have studied the density of states of a flat graphene sheet with a smooth curved portion with intrinsic curvature.

The massless Dirac equation in a curved space time is given by

$$i\gamma^{\mu}(\partial_{\mu}+\Omega_{\mu})\Psi=0, \tag{1}$$

where $\gamma^{\mu}=(\gamma^{0},v_{F}\gamma^{j})$, i=1,2. These curved γ matrices satisfy the anticommutation relations

$$\{\gamma^{\mu},\gamma^{\nu}\}=2g^{\mu\nu}(x), \tag{2}$$

and in general become functions of the point in space time $x=(t,\mathbf{r})$. $\Omega_{\mu}(x)$ is the spin connection of the spinor field that can be calculated using the tetrad formalism[24] and will be defined in the Appendix. In this work we will not consider time dependent shapes and from now on the time coordinate will be kept aside.

What is needed is a metric describing the curvature of the surface. We will study the general case of a smooth protuberance fitting without singularities in the average flat graphene sheet. We start by embedding a two-dimensional surface with polar symmetry in three-dimensional space (described in cylindrical coordinates). The surface is defined by a function $z(r)$ giving the height with respect to the flat surface $z=0$, and parametrized by the polar coordinates of its projection onto the $z=0$ plane. The metric for this surface is obtained as follows: We compute

$$dz^{2}=\left(\frac{dz}{dr}\right)^{2}dr^{2}\equiv\alpha f(r)dr^{2}, \tag{3}$$

and substitute for the line element

$$ds^{2}=dr^{2}+r^{2}d\theta^{2}+dz^{2}=(1+\alpha f(r))dr^{2}+r^{2}d\theta^{2}. \tag{4}$$

We will assume that the surface is asymptotically flat at long distances, so that f decays with r fast enough. We will also require f to go to zero sufficiently fast in $r=0$ so that the surface is smooth there. For clarity, we work out as an example the Gaussian bump shown in Fig. 1 defined by

$$z=A\exp(-r^{2}/b^{2}), \tag{5}$$

so that

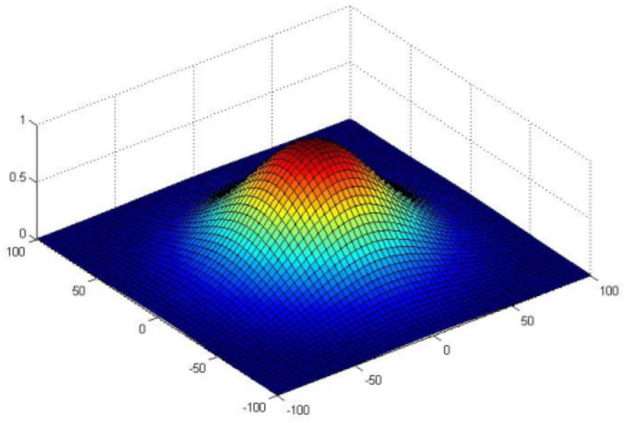

FIG. 1. (Color online) The smooth curved bump discussed in the text.

$$dz^{2}=\frac{A^{2}}{b^{4}}4r^{2}\exp(-2r^{2}/b^{2})dr^{2}, \tag{6}$$

which corresponds to Eq. (4) with

$$\alpha=(A/b)^{2},\quad f(r)=4(r/b)^{2}\exp(-2r^{2}/b^{2}).$$

The ratio of the height to the mean width of the Gaussian will be our perturbative parameter. Values of b of the order of 0.1—0.3 times the height A give bumps of magnitude and shape comparable with the ripples reported in Refs. 1 and 25.

The line element reads

$$ds^{2}=-(1+\alpha f)dr^{2}-r^{2}d\theta^{2}, \tag{7}$$

from where we can write the metric in a more usual form

$$g_{\mu\nu}=\begin{pmatrix}-(1+\alpha f(r)) & 0\\ 0 & -r^{2}\end{pmatrix}. \tag{8}$$

Since we are dealing with a problem with axial symmetry, we will work in polar coordinates. The Dirac Hamiltonian of the plane (flat) in polar coordinates can be written as

$$H_{flat}=\hbar v_{F}\begin{pmatrix}0 & \partial_{r}+i\frac{\partial_{\theta}}{r}+\frac{1}{2r}\\ \partial_{r}-i\frac{\partial_{\theta}}{r}+\frac{1}{2r} & 0\end{pmatrix}, \tag{9}$$

where, as discussed in the Appendix, a constant spin connection has been generated that is a "pure gauge" and can be rotated away by a different choice of local coordinates.[35] The calculation of the different geometric factors for the metric (7) is given in the Appendix. Adding them together we get the curved Hamiltonian

$$H_{curved} = \hbar v_F \begin{pmatrix} 0 & (1+\alpha f(r))^{-1/2}\partial_r + i\frac{\partial_\theta}{r} + A_\theta \\ (1+\alpha f(r))^{-1/2}\partial_r - i\frac{\partial_\theta}{r} + A_\theta & 0 \end{pmatrix}, \tag{10}$$

where the effective gauge potential is related to the coefficient of the spin connection computed in Eq. (A21) by

$$A_\theta = \frac{\Omega_\theta}{2r} = \frac{1-(1+\alpha f)^{-1/2}}{2r}. \tag{11}$$

Comparing Eq. (9) with Eq. (10) we can read that the curved bump has produced an effective Fermi velocity $\tilde{v}_r$ in the radial direction given by

$$\tilde{v}_r(r,\theta) = v_F(1+\alpha f(r))^{-1/2}, \tag{12}$$

and an effective magnetic field perpendicular to the graphene sheet given by

$$B_z = -\frac{1}{r}\partial_r(rA_\theta) = \frac{1}{4r}\frac{\alpha f'}{(1+\alpha f)^{3/2}}. \tag{13}$$

The magnitude of this effective magnetic field is estimated to be of the order of 0.5 to 2–3 T in the region spanned by the bump, compatible with the estimations given in Ref. 25, and it will play the same role in the issue of the weak localization of graphene as the effective magnetic fields discussed there and in Ref. 26.

We note that in general the effective Fermi velocity will be smaller in magnitude than the free one. For a general curved surface described in polar coordinates by $z=z(r)$, the effective Fermi velocity will be

$$v_r = \frac{v_0}{\sqrt{1+z'(r)^2}}. \tag{14}$$

In a most general case we will have the two components of the velocity changed but always to a smaller value.

In the next section we specify the method to compute the density of states through the electron Green's function. For this purpose it is more convenient to follow the Appendix and rewrite the Dirac equation in the form

$$\left[i\gamma^0\partial_0 + i\Gamma(\theta)\partial_r + i\Gamma'(\theta)\frac{\partial_\theta}{r} + V(r,\theta) \right]\Psi = 0, \tag{15}$$

which is the flat Dirac equation in polar coordinates in a sort of potential V given by

$$V(r,\theta) = i\Gamma(\theta)[1-(1+\alpha f)^{-1/2}]\left(\frac{1}{2r} - \partial_r\right), \tag{16}$$

where $\Gamma(\theta)=\gamma^1\cos\theta+\gamma^2\sin\theta$. This effective potential will be used in the next section to compute the local density of states of the system. We can read in it two different terms related with our previous discussion: the derivative term has its origin in the effective r-dependent Fermi velocity and the term proportional to $1/r$ comes from the effective gauge field.

III. GREEN'S FUNCTION IN A CURVED SPACE TIME: APPROXIMATIONS

We drop the polar coordinates for a moment to outline the procedure to obtain the Dirac propagator in a sort of perturbative expansion.

Since we will be interested in small deformations from the flat membrane, we will compute the first order correction to the "flat" propagator in the small parameter α. In our example, $\alpha=(A/b)^2$ is the (squared) height to length ratio of the Gaussian, so for typical ripples in graphene $\alpha\approx 0.01$, since this ratio is of the order of 0.1.[1]

The equation for the exact propagator in the curved space time is

$$i\gamma^\alpha e_\alpha^\mu(\partial_\mu + \Omega_\mu)G(x,x') = \delta(x-x')(-g)^{-1/2}, \tag{17}$$

where Ω_μ is the spin connection computed in Eq. (A21) and $\sqrt{-g}$ is the determinant of the metric given in Eq. (A7). Since the flat propagator equation is recovered when $\alpha=0$, expanding the left hand side to first order in α will give this flat equation plus a first order general term that we will call V. We can as well expand $(-g)^{-1/2}=1-\alpha f(x)$, and sending the f term to the left hand side we get an equation resembling the flat propagator equation in a sort of potential generated by the metric.

$$(i\gamma^\mu\partial_\mu + V)G(x,x') + \alpha f(x)\,\delta(x-x') = \delta(x-x'). \tag{18}$$

This equation can be solved by the usual pertubative expansion of G in a potential. Note that two approximations to order α are taking place: first, we expand the curved space exact equation for G to make it resemble the flat equation in a potential, and then we use a perturbative expansion in the potential to get the first order correction to G.

The solution for G is given by

$$G(x,x') = G_0(x-x') - G_0(x-x')\alpha f(x) + \int dx'' G_0(x,x'')V(x'')G_0(x'',x'). \tag{19}$$

We now proceed to use this expansion in our particular case. The determinant of the metric is just

$$g^{-1/2} = \frac{(1+\alpha f)^{-1/2}}{r} \approx \frac{1-\frac{\alpha f}{2}}{r}. \tag{20}$$

Expanding Eq. (16) to first order in α we get

$$V(r,\theta) = i\Gamma(\theta)\left[\frac{1}{2}\alpha f(r)\right]\left(\frac{1}{2r} - \partial_r\right). \tag{21}$$

Noting that the flat δ function in polar coordinates is $\delta(r-r')/r$, we can use Eq. (19) in polar coordinates to get the first order correction to the propagator.

Next we need the Dirac propagator in polar coordinates. We will get it by noting that the Dirac and Klein-Gordon propagators are related by

$$G_D^0 = D(x)G_{KG}^0, \tag{22}$$

where $D(x)$ is the Dirac operator. The Dirac operator in polar coordinates is

$$\gamma^0 E + i\left[\Gamma(\theta)\partial_r + \Gamma'(\theta)\frac{\partial_\theta}{r}\right], \tag{23}$$

where we have defined

$$\Gamma(\theta) = \gamma^1\cos(\theta) + \gamma^2\sin(\theta),$$

$$\Gamma'(\theta) = -\gamma^1\sin(\theta) + \gamma^2\cos(\theta). \tag{24}$$

The Klein-Gordon propagator in polar coordinates is

$$G_{KG}(r-r',E) = \frac{-i}{4}H_0(E|r-r'|), \tag{25}$$

where H_0 is the zeroth order Hankel function.[27] Applying Eqs. (22) and (23) we get

$$G_D(r-r',E) = \frac{-iE}{4}\gamma^0 H_0(E|r-r'|) - \frac{E}{4|r-r'|}H_1(E|r-r'|) \times[r\Gamma(\theta) - r'\Gamma(\theta')]. \tag{26}$$

Now we just use Eqs. (19) and (26), and the first order potential (21) to get the local density of states

$$\rho(E,\mathbf{r}) = -\frac{1}{\pi}\,\mathrm{Im}\,\mathrm{Tr}[G(E,\mathbf{r},\mathbf{r})\gamma^0]. \tag{27}$$

After two partial integrations we obtain the local density of states as

$$\rho(r',E) = g\frac{E}{2\pi}\frac{1}{(v_F\hbar)^2}\left(1 - \frac{\alpha f(r')}{2} + \frac{\alpha}{8}\int dr d\theta\,.\left\{4E^2 f(r) r\frac{r - r'\cos(\theta-\theta')}{[r^2 + r'^2 - 2rr'\cos(\theta-\theta')]^{1/2}}Y_1(E\Delta r)J_1(E\Delta r) - [2f'(r) + rf''(r)]Y_0(E\Delta r)J_0(E\Delta r)\right\}\right), \tag{28}$$

where g is the spin and valley degeneracy, $\Delta(r) \equiv |r-r'|$, and Y_i and J_i are Bessel functions.[27] We will analyze this result in the next section.

IV. RESULTS

The main result of this work is the confirmation of the fact that the morphology of the graphene samples is correlated with the electronic properties. In particular, the presence of ripples, irrespective of their origin, induces corrections to the density of states and will affect the transport properties. The analysis of this work is quite general and the results will apply to any smooth surface. We have considered as an example a Gaussian bump of an average spacial extent of 2–20 nm similar to the ripples described in Ref. 1 and 25. As can be read from Eq. (28) due to the Bessel functions the corrections to the local density of states (LDOS) show spacial oscillations whose frequency grows with the energy and whose amplitude decays with the distance as $(1/r)$. Figure 2 shows the correction to the LDOS induced by the shape of Fig. 1 with a mean width b of 50 Å and for an energy of E=0.1 eV. The color scale is indicated in the figure. Lighter (darker) color means a positive (negative) contribution with respect to the flat graphene sheet at the given energy. The maximal value of the correction related to the bare LDOS $\rho(E,r)/\rho_0(E,r)$ for a bump of a ratio $A/b \sim 0.1$ is of the order of 1%. If the height of the ripples goes up to 0.3, the maximal value of the correction to the LDOS due to the curved portion can reach 10%. Larger values are possible but they would correspond to higher values of our perturbative parameter α and made the result questionable. The bare LDOS being proportional to the energy (E) allows us to re-

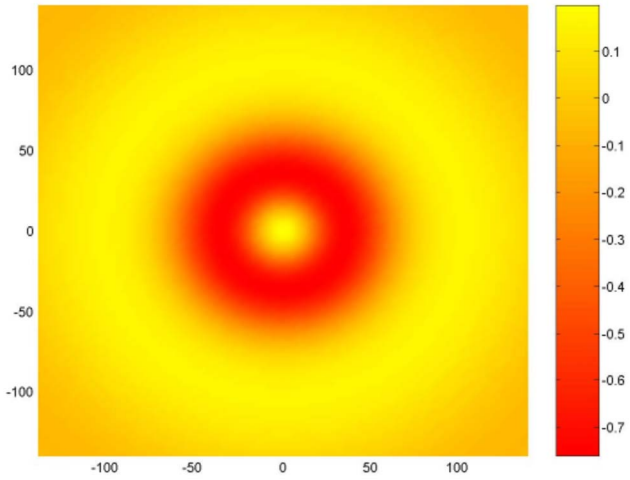

FIG. 2. (Color online) Effect of the curved bump of Fig. 1 on the local density of states of the graphene sheet.

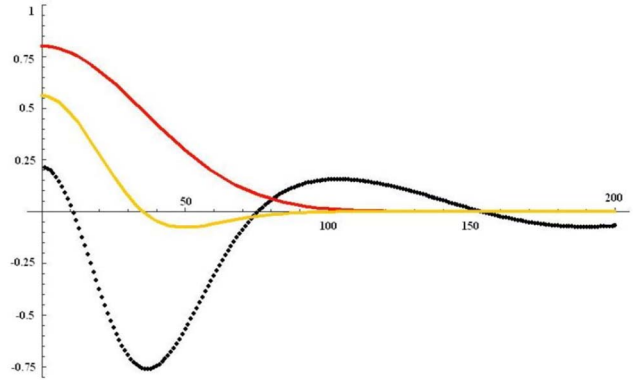

FIG. 3. (Color online) Correction to the density of states (dotted line) in arbitrary units, versus the shape of defect (red—upper line) and curvature of the defect (yellow—middle line) for a Gaussian bump of an average width of 50 Å.

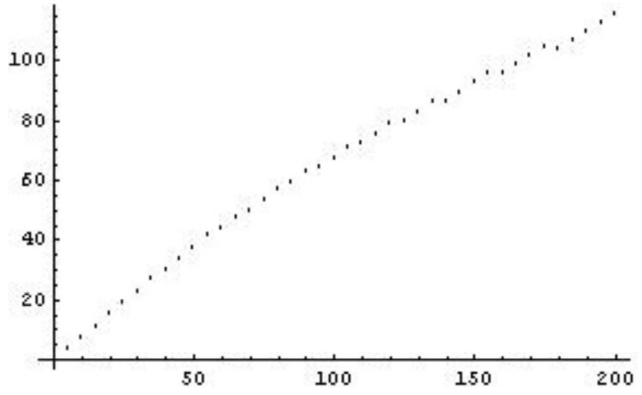

FIG. 4. Plot of the location of the maximal correction of the LDOS for a fixed energy as a function of the extension of the Gaussian bump.

late the correction obtained with the energy at which the experiment takes place.

At low energies the maximal absolute value of the correction is correlated with the zero of the curvature which, in the particular case of the Gaussian bump, coincides with the mean width $\sqrt{2}b$. Figure 3 shows the correction to the local density of states (dotted line) in arbitrary units, versus the shape of defect (red—upper line) and the curvature of the defect (yellow—middle line) for a Gaussian bump of an average width of 50 Å. The energy is 0.1 eV. The figure represents real space in polar coordinates. The horizontal axis is the r coordinate, while the vertical axis represents real height in the case of the upper line (shape of the Gaussian bump considered). The middle line (curvature) given in Eq. (A14) is not measured in units of length. Finally, the lowest curve gives the correction to the LDOS in arbitrary units. This results seems to be at odd with related works based on topological defects[25,26] or elasticity[14] that correlate the physical effect of curved portions with the actual value of the geometrical curvature.

We notice here that of the two effects of the curvature discussed in this work, only the effective magnetic field coming from the spin connection can be compared with previous works. In our case and in the general situation of having a smooth shape with axial symmetry, the effect of the effective gauge field vanishes at first order in perturbation theory and the corrections to the local density of states come exclusively from the spacial dependence of the Fermi velocity. This effect has not been noticed before because most of the previous works coupling the Dirac equation to curved space dealt either with spherical shapes where the correction to the Fermi velocity is constant and can be scaled out, or with conical shapes whose intrinsic curvature is accumulated at the apex singularity.

A discussion on the various gauge fields that arise in the physics of graphene and their physical consequences will be published elsewhere.[28]

For simplicity we have modeled the ripples with shapes that are axially symmetric and the axial symmetry is explicit in the results. More general shapes would made the calculation much more complicated without altering the main results.

We can observe in Figs. 2 and 3 that the maximal value of the correction to the LDOS is concentrated in the region spanned by the bump. In an STM experiment done on the curved surface the results on the LDOS plotted on the flat surface should resemble the rings of Fig. 2 and would be in a very precise correspondence with the morphology of the sample.

To verify the apparent pining of the maximal value of the correction to the zero of the curvature observed in Fig. 3 we have explored a set of Gaussian shapes with different widths. The result is plotted in Fig. 4. The correlation is good for the physical values of the bump from 2 to 5 nm (50 Å). Figure 5 shows the dependence of the correction to the LDOS with the energy. The four plots show the correction induced by the same bump of a width of 5 nm for growing values of the energy.

V. POSSIBLE EXPERIMENTAL CONSEQUENCES

We will here discuss the possible connection of this work with the recent experimental observations of electron-hole puddles of Ref. [10].

The main experimental facts that we have to address are the intrinsic disorder length scale of approximately 30 nm

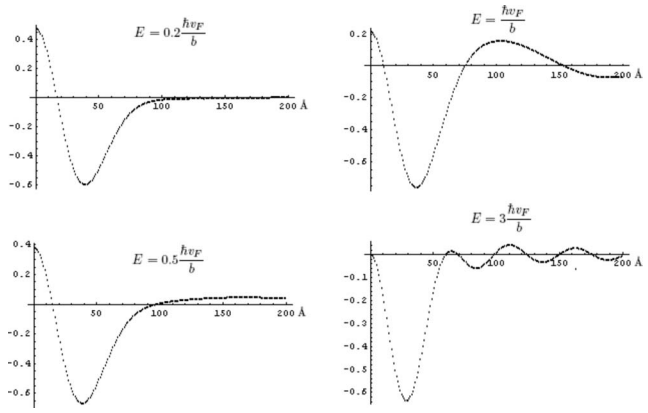

FIG. 5. Correction to the density of states of a bump of fixed width (50 Å) for different values of the energy.

and the magnitude of the density fluctuations of an average value $\Delta n \sim \pm 4.10^{10}$ cm^{-2} that can reach a maximum value of 10^{11} cm^{-2}.

In the experiment described in Ref. 10 the local inverse compressibility $\partial\mu/\partial n$ is measured as a function of a backgate voltage. In the case of having a flat graphene sheet this quantity can be computed analytically using the free dispersion relation and density of states, and it becomes more complicated when the latter is corrected due to the curvature.

Before entering in a more detailed analysis we can explain qualitatively the observation of Ref. 10 as follows: From our result of Sec. III we note that a variable correction to the density of states of the type shown in Eq. (28) causes a global, constant variation of the Dirac point E_D with respect to the charge neutrality point, because of the redistribution of the electronic charge when the density of states is modified locally (notice from Fig. 3 that the corrected LDOS is always lower than the flat one). This mechanism is the one proposed in Ref. 14 in a different context. An observation like the one done in Ref. 10 will see electron and hole puddles of the size of the ripples without the need to argue for charged impurities or other kinds of disorder. To give a number, we can estimate the density of carriers that we would need to induce to reach the Dirac point at a given position of the sample in this case as the integral of the correction of the density of states from some lower cutoff (of the order of −0.7 eV) to 0. In the case of the maximal correction we find this density to be of order $\Delta n \sim \pm 10^{11}$ cm^{-2}.

For a more quantitative discussion we consider a flat graphene sheet with some general E_D measured with respect to the charge neutrality point E_{cnp}, which we set to zero. The local density of states would be given in such a case by

$$\rho(E,r) = \frac{|E - E_D(r)|}{2\pi} \frac{g_S}{(\hbar v_F)^2}, \tag{29}$$

where $g_S=4$ is the degeneracy (spin and valley). When a voltage is applied, a density of carriers is induced locally, and thus the local chemical potential varies as well, though not linearly with the voltage. The induced number of carriers in this case can be computed as

$$n = \int_0^{\mu} dE \frac{|E - E_D|}{2\pi} \frac{g_S}{(\hbar v_F)^2} = \int_{-E_D}^{-E_D+\mu} dE \frac{|E|}{2\pi} \frac{g_S}{(\hbar v_F)^2}. \tag{30}$$

The integration yields, taking appropriate care of the signs due to the absolute value,

$$n = \frac{[\mathrm{sgn}(-E_D+\mu)(-E_D+\mu)^2 - \mathrm{sgn}(-E_D)E_D^2]g_S}{4\pi(\hbar v_F)^2}. \tag{31}$$

The rate of change $\partial n/\partial\mu$ is again $\rho(-E_D+\mu)$, and solving for μ in Eq. (31), substituting the value, and inverting, we obtain

$$\frac{\partial\mu}{\partial n} = \frac{\hbar v_F}{\left| \frac{n g_S}{\pi} - \frac{E_D^2\, \mathrm{sgn}(E_D) g_S^2}{4\pi^2(\hbar v_F)^2} \right|^{1/2}}, \tag{32}$$

which reduces to the formula given in Ref. 10 when $E_D=0$. We can see that if E_D is shifted from zero, the curve for the inverse compressibility keeps its shape but it is displaced in the n axis, as shown in the experiment.

However, there is an alternative interpretation of the displacement of the curves. Instead of having a variable E_{cnp} from point to point, we could explain the shift by having a variable v_F as predicted in this work. We consider now the curved case, in which in a qualitative first approximation we just use Eq. (32) where $v_F^0 \to v_F(r)$. We can see in Eq. (32) that this substitution has two effects: first, it makes $\partial\mu/\partial n$ to scale with $v_F(r)$, and also the divergence is displaced by an amount proportional to $(E_D/v_F(r))^2$, different from the flat case. The scaling effect provides an experimental test of the variable Fermi velocity. Extracting the value of $v_F(r)$ from the shape of the curves at each point we can get a corrected map for E_D. We have analyzed carefully the experimental data of Ref. 10 to check this issue but the precision is not enough to deduce the change in the slope of the curves from point to point. Perhaps this effect can be tested in angle resolved photoemission experiments.

A related comment concerns the spatial variation of the Fermi velocity obtained in this work. Different ripple sizes randomly distributed over the sample will give rise to a landscape of Fermi velocities that will directly account for the size of the inhomogeneities reported. We note that the effective Fermi velocity is the (only) fitting parameter used in Ref. 10

VI. CONCLUSIONS AND DISCUSSION

We have studied the effect of curvature on the electronic properties of a graphene sheet as due to the spinor nature of the electron wave function. With complete generality we have seen that the curvature of the graphene sheet has two distinct effects with physical consequences. First the covariant derivative induces an effective magnetic field (the spin connection) that depends on the shape of the curved surface. This effect has been discussed before in the literature and can be understood in many ways. The second effect is even more interesting and comes from the curved Pauli matrices. They modify the Fermi velocity that becomes a function of the point on the graphene surface and is always lower than the free velocity. This is not to be confused with the renormalization of the Fermi velocity induced by electron-electron interactions[29] or disorder[7,30] where the Fermi velocity becomes effectively a function of the energy. This effect has not been noticed before because most of the previous works coupling the Dirac equation to curved space dealt either with spherical shapes where the correction to the Fermi velocity is constant and can be scaled out, or with conical shapes whose intrinsic curvature is accumulated at the apex singularity.

To model the ripples observed in graphene we have applied the formalism to study a smooth surface with local curvature that is asymptotically flat. We have studied the

changes in the density of states by computing the electronic Green's function in the presence of the curved bump. The effective potential generated by the curvature induces oscillations in the local density of states that affect significantly the region spanned by the bump. The potential couples to the electronic Dirac equation as a gauge field with two parts. One can be identified with an effective non-Abelian magnetic field of the type described previously associated with topological defects or external charges. This part does not contribute to the LDOS to first order in or perturbative expansion due to the traces over the gamma matrices. It will nevertheless affect other observables and will generate a density of states in nonperturbative calculations of the type recently presented in Ref. 31. The second piece of the effective potential represents a gauge field with a derivative coupling and comes from the modified Fermi velocity. This is the one producing the results presented in this work. A conservative estimate gives a relative correction to the flat density of the order of 0.5 to a few percent at the energies usually explored with STM probes that should be able to correlate the morphology with the predicted correction. The estimated corrections due to curvature are considerable larger than the ones recently obtained with the theory of elasticity.[14] They are also different: in most cases due to the traces over the gamma matrices, the correction to the density of states that would come from the spin connection vanishes and what remains arises exclusively from the derivative term in the potential (the correction to the Fermi velocity). The space variation of the Fermi velocity induced by the curvature provides an alternative explanation for the charge anisotropies observed in Ref. 10 and reinforces the effect. We propose a mechanism to disentangle the two effects (a space dependent chemical potential versus a space dependent Fermi velocity) that would provide an experimental test of the curvature effects described in this work.

The mechanism proposed based on the variable Fermi velocity due to the curvature of the sheets can be distinguished from other mechanisms by the fact that a variable v_F in addition to displace the position of the curves would change their slope at different positions of the sample providing an experimental test of the model discussed in this work.

From the discussion done in this paper it is clear that a part of the described modification of the Fermi velocity can be transferred by a gauge transformation to the vector potential and vice versa. Any formulation will produce the same results when computing observable quantities. In this respect we should not identify the effective Fermi velocity with any tight binding parameter. As happens in general relativity, curvature means interactions. The Fermi velocity measured in the photoemission experiments or by any other means is the result of the bare value and the interactions so there is no paradox here.

The presence of a random distribution of curved portions as the one discussed in this work will affect the transport properties of the system. In this case the effective magnetic field will play a role similar to the one discussed in the literature.[32] This issue is currently under investigation and it will be reported in a different work.

The concrete calculations presented in this work are a simplification. To model real graphene samples we would need either several bumps located at appropriate distances or a random distribution of them. We believe that if the density of curved portions is not high we will obtain a landscape of Fermi velocities that could be observed with STM and experiments in this direction are actually in course.[33] As mentioned in Sec. III, the assumed axial symmetry of the curved shapes allows us to present analytical results. The formalism can be applied to more general shapes where numerical calculations would provide similar results on the density of states.

ACKNOWLEDGMENTS

We thank Andre Geim for a careful reading of the manuscript and for making many useful suggestions, Amir Yacoby and Jens Martin for sharing their experimental data with us, and Jens Martin specially for his patience in providing details of their analysis. We also thank J. J. Palacios and F. Guinea for useful conversations. Support by MEC (Spain) through Grant No. FIS2005-05478-C02-01 and by the European Union Contract No. 12881 (NEST) is acknowledged. We thank A. Geim for suggesting us to explore in this direction. We thank A. Yacobi and J. Martin for kindly providing their data and explaining them to us.

APPENDIX: GAUSSIAN BUMP: GEOMETRIC FACTORS

The behavior of spinors in curved spaces is more complicated than that of scalar or vector fields because their Lorentz transformation rules do not generalize easily to arbitrary coordinate systems. Instead of the usual metric $g_{\mu\nu}$ we must introduce at each point X described in arbitrary coordinates, a set of locally inertial coordinates ξ_X^a and the fielbein fields $e_\mu^a(x)$, a set of orthonormal vectors labeled by a that fixes the transformation between the local and the general coordinates

$$e_\mu^a(X) \equiv \left.\frac{\partial \xi_X^a(x)}{\partial x^\mu}\right|_{x=X}. \tag{A1}$$

We will later compute the fielbein for our particular metric. The curved space gamma matrices $\gamma^\mu(x)$ satisfying the commutation relations

$$\{\gamma_\mu \gamma_\nu\} = 2g_{\mu\nu} \tag{A2}$$

are related with the constant, flat space matrices γ^μ by

$$\gamma^\mu(x) = e_a^\mu \gamma_a. \tag{A3}$$

The spin connection $\Omega_\mu(x)$ is defined from the fielbein by

$$\Omega_\mu(x) = \frac{1}{4}\gamma_a \gamma_b e_\lambda^a(x) g^{\lambda\sigma}(x) \nabla_\mu e_\sigma^b(x), \tag{A4}$$

with

$$\nabla_\mu e_\sigma^a = \partial_\mu e_\sigma^a - \Gamma_{\mu\sigma}^\lambda e_\lambda^a, \tag{A5}$$

where $\Gamma_{\mu\sigma}^\lambda$ is the usual affine connection which is related to the metric tensor by[34]

$$\Gamma_{\mu\sigma}^\lambda = \frac{1}{2} g^{\nu\lambda}\left(\frac{\partial g_{\sigma\nu}}{\partial x^\mu} + \frac{\partial g_{\mu\nu}}{\partial x^\sigma} - \frac{\partial g_{\mu\sigma}}{\partial x^\nu}\right). \tag{A6}$$

Finally, the determinant of the metric needed to define a scalar density Lagrangian is given by

$$\sqrt{-g} = [\det(g_{\mu\nu})]^{1/2} = \det[e^a_\mu(x)]. \tag{A7}$$

Before going to the computation of the geometric factors related with the metric of Eq. (8) we will apply the formalism to the flat space in polar coordinates that will help us to clarify the physical discussion later. The two-dimensional metric of the flat space in polar coordinates is

$$g_{\mu\nu} = \begin{pmatrix} 1 & 0 \\ 0 & r^2 \end{pmatrix}. \tag{A8}$$

The affine connection $\Gamma^\lambda_{\mu\nu}$ that only depends on the metric is

$$\Gamma^r_{rr} = 0, \quad \Gamma^r_{\theta\theta} = -r, \quad \Gamma^\theta_{r\theta} = \frac{1}{r}. \tag{A9}$$

Despite the fact that the spin connection appears to be nontrivial, the Riemann curvature which is the "observable" quantity and does not depend on the choice of coordinates is zero as corresponds to flat space.

The fielbein fields e^a_μ satisfy

$$g_{\mu\nu} = e^a_\mu e^b_\nu \eta_{ab}, \tag{A10}$$

where η_{ab} is the identity matrix in two dimensions.

This relation does not fix e^a_μ uniquely. There are two natural choices: one is

$$e^a_\mu = (e^\mu_a)^{-1} = \begin{pmatrix} 1 & 0 \\ 0 & r \end{pmatrix} \tag{A11}$$

and the other one is

$$e^a_\mu = \begin{pmatrix} \cos\theta & -r\sin\theta \\ \sin\theta & r\cos\theta \end{pmatrix}. \tag{A12}$$

The two choices can be visualized as associated with flat local frames that at points of constant r have fixed directions (last) or rotate with the polar angle (first). The first choice leaves the gamma matrices as in the Cartesian plane and induces a constant gauge connection whose "associated magnetic field" is obviously zero.

The second choice transforms the flat gamma matrices and does not induce a gauge connection.

Let us now compute the geometric factors related with the metric of Eq. (8): The affine connection $\Gamma^\lambda_{\mu\nu}$ for the metric (8) is

$$\Gamma^r_{rr} = \frac{\alpha f'}{2(1+\alpha f)}, \quad \Gamma^r_{\theta\theta} = -\frac{r}{1+\alpha f}, \quad \Gamma^\theta_{r\theta} = \frac{1}{r}, \tag{A13}$$

where $f' = df/dr$, and the rest of the elements are zero or related by symmetry.

The geometrical (Gaussian) curvature K of the shape given by Eq. (5) is

$$K(r) = \frac{\alpha f'(r)}{2r(1+\alpha f(r))^2}. \tag{A14}$$

The fielbein fields e^a_μ satisfy

$$g_{\mu\nu} = e^a_\mu e^b_\nu \eta_{ab}, \tag{A15}$$

where $g_{\mu\nu}$ is our metric given in Eq. (8) and

$$\eta_{ab} = \begin{pmatrix} -1 & 0 \\ 0 & -1 \end{pmatrix}. \tag{A16}$$

We choose the e^a_μ to be

$$e^1_r = (1+\alpha f)^{1/2}\cos\theta, \quad e^1_\theta = -r\sin\theta,$$

$$e^2_r = (1+\alpha f)^{1/2}\sin\theta, \quad e^2_\theta = r\cos\theta, \tag{A17}$$

which reduce to the flat set (A12) when $\alpha = 0$. Now we can compute the spin connection coefficients

$$\omega^{ab}_\mu = e^a_\nu(\partial_\mu + \Gamma^\nu_{\mu\lambda})e^{b\lambda}, \tag{A18}$$

which are found to be

$$\omega^{12}_\theta = 1 - (1+\alpha f)^{-1/2}, \tag{A19}$$

the rest being zero or related by symmetry (the spin connection ω is antisymmetric in the upper indices).[34]

The spin connection

$$\Omega_\mu = \tfrac{1}{8}\omega^{ab}_\mu[\gamma_a, \gamma_b] \tag{A20}$$

turns out to be

$$\Omega_r = 0, \quad \Omega_\theta = \frac{1-(1+\alpha f)^{-1/2}}{2}\gamma^1\gamma^2. \tag{A21}$$

Finally, the Dirac equation coupled to the curved surface is

$$i\gamma^\mu e^\mu_a(\partial_\mu + \Omega_\mu)\psi = 0. \tag{A22}$$

Substituting all previously computed elements and with some more algebra, we can cast Eq. (1) into the form

$$\left[i\gamma^0\partial_0 + i\Gamma(\theta)\partial_r + i\Gamma'(\theta)\frac{\partial_\theta}{r} + V(r,\theta) \right]\Psi = 0, \tag{A23}$$

which is the flat Dirac equation in a sort of potential V given by

$$V(r,\theta) = i\Gamma(\theta)[1-(1+\alpha f)^{-1/2}]\left(\frac{1}{2r} - \partial_r\right). \tag{A24}$$

[1] J. C. Meyer, A. K. Geim, M. I. Katsnelson, K. S. Novoselov, T. J. Booth, and S. Roth, Nature (London) **446**, 60 (2007).
[2] J. C. Meyer, A. K. Geim, M. I. Katsnelson, K. S. Novoselov, D. Obergfell, S. Roth, C. Girit, and A. Zettl, Solid State Commun. **143**, 101 (2007).
[3] E. Stolyarova, K. T. Rim, S. Ryu, J. Maultzsch, P. Kim, L. E. Brus, T. F. Heinz, M. S. Hybertsen, and G. W. Flynn, Proc. Natl. Acad. Sci. U.S.A. **104**, 9211 (2007).
[4] M. Ishigami, J. H. Chen, W. G. Cullen, M. S. Fuhrer, and E. D. Williams, Nano Lett. (to be published).
[5] R. Tamura and M. Tsukada, Phys. Rev. B **49**, 7697 (1994).
[6] J. C. Charlier and G. M. Rignanese, Phys. Rev. Lett. **86**, 5970 (2001).
[7] J. González, F. Guinea, and M. A. H. Vozmediano, Phys. Rev. B **63**, 134421 (2001).
[8] A. Cortijo and M. A. H. Vozmediano, Europhys. Lett. **77**, 47002 (2007).
[9] A. Cortijo and M. A. H. Vozmediano, Nucl. Phys. B **763**, 293 (2007).
[10] J. Martin, N. Akerman, G. Ulbricht, T. Lohmann, J. H. Smet, K. von Klitzing, and A. Yacoby, arXiv:cond-mat/0705.2180 (unpublished).
[11] M. I. Katsnelson, K. S. Novoselov, and A. K. Geim, Nat. Phys. **2**, 620 (2006).
[12] Y. Lu, M. Munoz, C. S. Steplecaru, C. Hao, M. Bai, N. García, K. Schindler, and P. Esquinazi, Phys. Rev. Lett. **97**, 076805 (2006).
[13] T. O. Wehling, A. V. Balatsky, M. I. Katsnelson, A. I. Lichtenstein, K. Scharnberg, and R. Wiesendanger, Phys. Rev. B **75**, 125425 (2007).
[14] A. Castro-Neto and E. Kim, arXiv:cond-mat/0702562 (unpublished).
[15] J. González, F. Guinea, and M. A. H. Vozmediano, Phys. Rev. Lett. **69**, 172 (1992).
[16] J. González, F. Guinea, and M. A. H. Vozmediano, Nucl. Phys. B **406**, 771 (1993).
[17] J. González, F. Guinea, and M. A. H. Vozmediano, Int. J. Mod. Phys. B **7**, 4331 (1993).
[18] V. A. Osipov and D. Kolesnikov, Rom. J. Phys. **50**, 457 (2005).
[19] D. Kolesnikov and V. A. Osipov, Eur. Phys. J. B **49**, 465 (2006).
[20] C. Furtado and F. Moraes, Phys. Lett. A **188**, 394 (1994).
[21] I. E. Dzyaloshinskii and G. E. Volovik, Ann. Phys. (N.Y.) **125**, 67 (1980).
[22] M. O. Katanaev and I. V. Volovich, Ann. Phys. (N.Y.) **216**, 1 (1992).
[23] A. Cortijo and M. A. H. Vozmediano, Proceedings of the Graphene Conference, MPI PKS Dresden, September 2006 (unpublished).
[24] N. D. Birrell and P. C. W. Davis, *Quantum Fields in Curved Space* (Cambridge University Press, Cambridge, 1982).
[25] S. V. Morozov, K. S. Novoselov, M. I. Katsnelson, F. Schedin, L. A. Ponomarenko, D. Jiang, and A. K. Geim, Phys. Rev. Lett. **97**, 016801 (2006).
[26] A. F. Morpurgo and F. Guinea, Phys. Rev. Lett. **97**, 196804 (2006).
[27] I. S. Gradshteyn and I. M. Ryzhik, *Tables of Integrals, Series and Products* (Academic, New York, 1980).
[28] A. Cortijo, F. de Juan, and M. A. H. Vozmediano (unpublished).
[29] J. González, F. Guinea, and M. A. H. Vozmediano, Nucl. Phys. B **424**, 595 (1994).
[30] T. Stauber, F. Guinea, and M. A. H. Vozmediano, Phys. Rev. B **71**, 041406(R) (2005).
[31] D. V. Khveshchenko, arXiv:0705.4105 (unpublished).
[32] D. Khveshchenko and A. Yashenkin, Phys. Lett. A **309**, 363 (2003).
[33] E. Andrei (private communication).
[34] S. Weinberg, *Gravitation and Cosmology: Principles and Applications to the General Theory of Relativity* (Wiley, New York, 1972).
[35] We can see that the effective magnetic field generated by this potential is zero.